Nephrol Dial Transplant (2009) 24: 2038–2044
doi: 10.1093/ndt/gfn743
Advance Access publication 21 January 2009

Original Articles

NDT
Nephrology Dialysis Transplantation

CRIM1 is localized to the podocyte filtration slit diaphragm of the adult human kidney

Jenny Nyström[1], Kjell Hultenby[2], Sara Ek[3], Jonas Sjölund[4], Håkan Axelson[4], Karin Jirström[4], Moin A. Saleem[5], Kristina Nilsson[4] and Martin E. Johansson[4]

[1]Department of Nephrology, Göteborg University, Gothenburg, [2]Division of Electron Microscopy, Karolinska University Hospital, Huddinge, Karolinska Institutet, Stockholm, [3]Lund University, Department of Immunotechnology, CREATE Health, BioMedical Center, [4]Department of Laboratory Medicine, Center for Molecular Pathology, Lund University, University Hospital MAS, Malmö, Sweden and [5]Academic Renal Unit, University of Bristol, Bristol, UK

Correspondence and offprint requests to: Martin E. Johansson; E-mail: martin.johansson@med.lu.se

Abstract

Background. CRIM1 is a plasma membrane bound protein containing six cysteine-rich repeats (CRR). Through these, CRIM1 has been shown to interact with a subgroup of the TGF-β superfamily, the bone morphogenic proteins (BMP) isoforms 2, 4 and 7. The probable action is to modulate the signalling properties of these factors. CRIM1 has also been shown to regulate the release of VEGFA by podocytes during renal organogenesis. Knock-out studies in mice have shown that CRIM1 is critically involved in the development of the central nervous system, eye and kidney. Replacement of CRIM1 with a defective version leads to renal dysgenesis and perinatal death. We have analysed the distribution of CRIM1 in adult human renal tissue.

Methods. To this end, we have used immunofluorescence, immunohistochemistry and immunoelectron microscopy. We performed western blotting for the CRIM1 protein, using lysates from isolated glomerular podocytes and human renal tissue homogenate. By using quantitative PCR, we compared the CRIM1 mRNA levels in podocytes, human renal tissue homogenate, primary human renal proximal tubular epithelial cells and primary human pulmonary artery smooth muscle cells.

Results. The results show that in the human adult kidney, CRIM1 is mainly expressed in the glomerular podocytes and is associated with the insertional region of the filtration slit diaphragm (SD) of the podocyte pedicles.

Conclusions. CRIM1 is a protein that should be added to the list of proteins associated with the podocyte filtration SD and with the probable action of modulating BMP and VEGFA signalling.

Keywords: bone morphogenic protein; filtration slit membrane; immunoelectron microscopy; podocyte

Introduction

CRIM1 is an *N*-glycosylated plasma membrane bound protein with a large extracellular moiety containing six von Willebrand-like, cysteine-rich repeats (CRR) and an IGF-binding protein motif. It has been proposed that a minor proportion of CRIM1 also appears as a cleaved extracellular molecule [1,2]. In the adult human, CRIM1 mRNA has been detected in several organs, although the highest levels were seen in the placenta, followed by the kidney [1].

The biological significance of CRIM1 during development has been firmly established. Studies conducted in zebrafish show aberrant development of the somites and vascular tissues when CRIM1 was knocked down [3]. Studies in mice have demonstrated the importance of CRIM1 for the development of the eye, the central nervous system and the kidney [4–6].

In the developing kidney, the presence of CRIM1 was detected by *in situ* hybridization, as early as during the metanephric stage where expression was seen in the ureteric bud, the early condensing mesenchyme and the comma shaped bodies [7]. By creating a gene-trap mouse line, where a truncated hypomorph of CRIM1 was allowed to be developmentally expressed, it was shown that the transgene was expressed in the glomerular epithelial cells, podocytes, mesangial cells, urothelium and vascular pericytes of the arterial vasculature [4,5].

Functionally, it was demonstrated that the bi-allelic form of the hypomorph CRIM1 resulted in perinatal death due to multiple organ defects and renal dysgenesis. The most pronounced disturbance was seen in the glomerulus, which demonstrated mesangiolysis, podocyte foot process effacement and dilation of the capillary loops. CRIM1 has also been implicated in angiogenesis, since it is required for the tube formation of capillary endothelial cells *in vitro* and is expressed in the endothelial lining of blood vessels *in vivo* [8].

The structure of CRIM1 makes it similar to other developmentally important proteins, such as vertebrate chordin and gremlin, the short gastrulation protein (sog) and kielin of *Drosophila* and uterine sensitization associated gene-1 (USAG-1) [9–13]. These are known to interact via their CRR domains with members of the TGF-β superfamily, more specifically the bone morphogenic proteins (BMP). In the mammalian kidney, the TGF-β superfamily plays a central role in disease as well as during renal development. TGF-β is generally regarded as the main profibrogenic agent, mediating the interstitial and glomerular fibrosis, which is the common final endpoint of most chronical renal diseases [14].

The BMP family has a crucial role in renal development and renal function postnatally. The BMP isoforms 2–7 are directly involved in the development of the kidney. Knock-out studies in mice demonstrated early embryonic lethality (BMP 2, 4 knock-out) or postnatal death (BMP 7 knock-out). All phenotypes showed a pronounced renal dysgenesis. No renal abnormality was detected if BMP3 and 6 were inactivated.

Much focus has been devoted to the isoform BMP7. In several experimental animal models of acute and chronic renal disease, BMP7 has been shown to reduce the inflammatory and fibrogenic processes that would otherwise lead to renal damage [15,16].

It has been convincingly shown in COS-1 cells that CRIM1 interacts with the pre-protein forms of BMP2, 4 and 7, tethering the inactive proforms of these factors to the extracellular face of the plasma membrane [2]. Whether this is the general mode of action by CRIM1 in other cell types, such as in the placenta or kidney, still remains to be elucidated. Little is known regarding the expression of known CRIM1 ligands in the human adult kidney. BMP7 has been localized mainly to the distal nephron, BMP2 expression has been said to be downregulated in adult kidneys and data are lacking as to the distribution of BMP4 [17,18]. It has also been shown that CRIM1 is able to interact with VEGFA, suggesting that CRIM1 modulates the delivery of VEGFA from the podocytes to the glomerular endothelial cells, thus regulating the release of this growth factor from the site of production [5]. The podocytes and glomerular endothelial cells are among the few cell types that continuously express VEGFA throughout life [19].

The exact localization of CRIM1 in the adult human kidney is still unknown. To this end we analysed human renal tissues for the presence of CRIM1, using a combination of immunohistochemical techniques, and the comparison of the expressional levels of CRIM1 mRNA in human glomerular podocytes, renal tissue homogenate, primary human renal proximal tubular cells and primary human pulmonary artery smooth muscle cells. We also compared the protein levels of CRIM1 in protein lysates from podocytes and human renal homogenate.

Materials and methods

Cell culture

A conditionally immortalized human podocyte cell line was obtained, the characteristics of which have been described in detail elsewhere [20]. In brief, isolated podocytes have been transfected with the catalytic subunit of the human telomerase gene and a temperature-sensitive mutant of the SV-40 large T-antigen. At the 'permissive' temperature of 33°C, the podocytes proliferate rapidly, driven by the SV-40 T-antigen. A subsequent thermoswitch to 37°C inactivates the T-antigen and instead induces growth arrest and differentiation of the podocytes, which express marker genes of differentiated podocytes such as synaptopodin, α-actinin-4 and CD2AP. The cells were grown in RPMI 1640 (Sigma, St Louis, MO, USA) with 10% fetal calf serum and addition of insulin-transferrin-selenium 100× stock solution (Invitrogen Inc, Carlsbad, CA, USA) to a final concentration of 1×. After 16 days at 37°C, the cells were harvested for standard protein extraction. Primary human renal proximal tubular cells (RPTEC) were obtained from Cambrex Bio Science (Walkersville MD, USA). The primary human pulmonary artery smooth muscle cells (HPASMC) were obtained from ScienceCell Research Laboratories (San Diego, CA, USA). Both cell systems were cultured according to the instructions of the respective manufacturers.

Immunohistochemistry

Sections of formalin fixed and paraffin embedded renal tissue, thickness 4 μm, were deparaffinized using xylene and graded ethanol for rehydration according to standard protocols. Human placenta was included as an additional positive control. Antigen retrieval was performed by boiling in a 10 mM citrate buffer, pH 6. The tissue sections were incubated by two separate antisera to CRIM1, one produced in chicken (Human Proteome Resource, HPR www.hpr.se /Kind gift from Professor Carl Borrebäck, Lund University) and one from rabbit origin (Atlas antibodies, Stockholm, Sweden). Also CRIM1 antibodies from Santa Cruz (sc-73860, Santa Cruz Biotechnology, Santa Cruz, CA, USA) and R & D systems (MAB1917, R & D systems, Abingdon, UK) were evaluated for immunohistochemistry, although the latter two sera had not been primarily developed for immunohistochemistry. Staining was detected using the Envision system and DAKO TechMate 500 staining equipment, according to the instructions of the manufacturer (DAKO, Copenhagen, Denmark). For nuclear counterstaining haematoxylin was used. As negative control, the primary antibody was omitted. Ethical permission was obtained from the Ethics Committee at Lund University (LU 289-07).

Immunofluorescence

Renal tissue was embedded in Tissue Tek cryo mountant (Sakura Finetek, Tokyo, Japan). Sections of 8 μm thickness were cut and allowed to dry overnight. The sections were fixed for 5 min in methanol having a temperature of −20°C. After blocking with 3% BSA in 10 mM PBS, the sections were incubated with a primary rabbit antibody against CRIM1 overnight at 8°C, at a dilution of 1:200 (Atlas antibodies). Following washing, a secondary goat anti rabbit antibody was applied at a dilution of 1:200 (Alexa fluor 488 goat anti rabbit, Invitrogen).

Immunoelectron microscopy (iEM)

Tissues used for immunoelectron microscopy (iEM) were fixed in 1% paraformaldehyde and 0.5% glutaraldehyde (GA), in a 0.1 M phosphate buffer. The tissues were dehydrated with methanol and embedded in Lowicryl K11M (Chemische Werke Lowi GmbH, Waldkraiburg, Germany) as described elsewhere [21]. The specimens were cut into ultrathin sections (60 nm) with a diamond knife and mounted on carbon/formvar nickel grids. To minimize non-specific labelling, grids were incubated in 2% bovine serum albumin (BSA, fraction IV) and 2% gelatin in a 0.1 M phosphate buffer at pH 7.4 for 2 h at room temperature followed by incubation overnight with anti-CRIM1 antibodies, diluted 1: 20 in a buffer containing 0.1% BSA and 0.1% gelatin (Atlas antibodies). After rinsing, the sections were incubated with protein A conjugated with 10 nm colloidal gold (Amersham Pharmacia Biotech, Little Chalfont, England) diluted 1:100 in the same buffer as for a primary antibody for 2 h at room temperature. The grids were then rinsed in a 0.1 M phosphate buffer and post-fixation was performed in 2% GA in a 0.1 M phosphate buffer for 20 min. The specimens were contrasted with 4% uranyl acetate followed by Reynold's lead citrate. The sections were examined in a LEO 906 transmission microscope (LEO Electron Microscopy Ltd, Cambridge, England) at 80 kV, and digital images were taken using a Morada camera (Soft Imaging System, GmbH, Münster, Germany). The number of gold particles over different compartments, i.e. podocytes, glomerular basement membrane (GBM), endothelial cells and mesangial matrix were

Table 1. Sequences of the DNA primers used in real-time quantitative PCR experiments

Gene	Forward (5′-3′)	Reverse (5′-3′)
CRIM1	TGCTATGGAGAA GGGTATTCCTTT	GGCCAGTGAGC AAATTGAAAA
SDHA	TGGGAACAA GAGGGCCATCTG	CCACCACTGCA TCAAATTCATG
YWHAZ	ACTTTTGGTACA TTGTGGCTTCAA	CCGCCAGGAGG ACAAACCAGTAT
UBC	ATTTGGGTC GCGGTTCTTG	TGCCTTGACA TTCTCGATGGT

counted on printed images. The area in podocyte was limited by drawing a line parallel with the GBM and 2 μm into the podocyte [22]. The area of different compartments was calculated using point counting using 1 and 2 cm square lattices according to Weibel [23]. A pilot study was performed to determine the number of pictures needed for an appropriate sample using cumulative mean plot for evaluation. Thus, 20 different images representing the capillary loop and 5 images representing mesangium matrix were collected.

Real-time quantitative PCR (Q-PCR)

The relative gene expression levels of CRIM1 in two individual cultures of immortalized podocytes were compared to the expressional levels of CRIM1 in whole kidney RNA from two human kidneys, HPASMC and RPTEC. This was performed by use of real-time quantitative PCR (Q-PCR) based on two-step SYBR green I chemistry.

Total RNA was extracted from cells or renal tissue using TRIzol reagent (Invitrogen) according to the manufacturer's instructions. Samples of 2 μg were subjected to DNase treatment and washed. Synthesis of cDNA was performed using random hexamers and Superscript II RT enzyme according to the manufacturer's instructions (Invitrogen). The resulting cDNA was used as a template in Q-PCR reactions using SYBR green Master Mix (Applied Biosystems, Foster City, CA, USA) according to the manufacturer's recommendations. The amplifications were run on a Gene Amp 7300 Sequence detector (Applied Biosystems), using two temperature cyclings (10 min 95°C, 40 cycles of 95°C for 15 s and 60°C for 60 s). Real-time detection of the PCR product was performed using the SYBR green master mix (Applied Biosystems), and all reactions were performed in triplicates. For relative quantification of mRNA expressional levels, we used the comparative C_T method and data were normalized to the expression of three reference genes (SDHA, YWHAZ and UBC) [24]. All Q-PCR primers were designed using the Primer Express software from Applied Biosystems. The sequences for the PCR primers used are given in Table 1.

Western blot analysis

The protein concentrations were determined by using the BCA Protein Assay Reagent kit (Pierce, Rockford, IL, USA). For western blotting, 20 μg of protein was separated on a 12% SDS-PAGE and transferred to Hybond ECL nitrocellulose membranes (Amersham Biosciences, Little Chalfont, UK). The membranes were incubated with primary anti-human CRIM-1 1:200 (R & D systems, Abingdon, UK) or anti GAPDH 1:2000 (Chemicon-Millipore, Nodinge, Sweden) antibodies followed by peroxidase-conjugated anti-mouse 1:5000 (Amersham Biosciences) antibody. The proteins were detected using enhanced chemiluminescence detection system (ECL+ plus) reagent (Amersham Biosciences) according to the manufacturer's instructions and exposed on ECL Hyper Film (Amersham Biosciences).

Results

Immunohistochemistry

The results of immunohistochemistry using the CRIM1 antiserum from Atlas antibodies performed on formalin-fixed and paraffin-embedded renal tissue is shown in Figure 1A. Linear staining can be seen in a pattern that is typical for either the glomerular basal membrane, the podocyte pedicles or to both of these structures. The mesangial areas were negative with respect to staining as well as the tubular, interstitial and vascular compartments of the kidney. Also, the chicken antibody from HPR worked well and resulted in similar staining patterns. The sera from Santa Cruz and R & D systems failed to produce a signal in renal tissue and also in human placenta that was used as a positive control (data not shown).

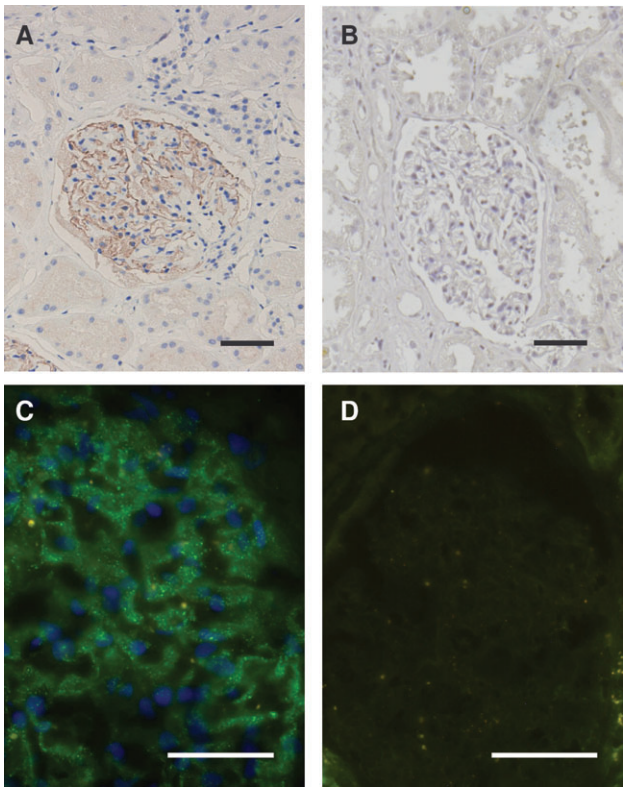

Fig. 1. (**A**) Section of formalin fixed normal human kidney stained with a rabbit polyclonal antibody directed against CRIM1 at a dilution of 1:200. Magnification 200×. (**B**) Control section, where the primary antibody was omitted and replaced by preimmune serum. Magnification 200×. Scale bar represents 50 μm. (**C**) Immunofluorescence staining pattern of CRIM1 in a glomerulus from fresh frozen human renal tissue stained with a rabbit polyclonal antibody against CRIM1, at a dilution of 1:100, showing a granular serpentine staining pattern indicative of antigens with podocyte or glomerular basal membrane origin. Nuclei have been counterstained by use of DAPI. Magnification 500×. (**D**) Control section, where the primary antibody as well as DAPI was omitted and replaced by preimmune serum and Vectashield mounting medium only. Magnification 500×. Scale bar represents 40 μm.

Immunofluorescence

The results of immunofluorescence of fresh frozen and methanol fixed tissues can be seen in Figure 1C. It basically shows a similar staining pattern, but with the additional information that the basal membrane staining is rough and granular in a serpentine fashion. This staining pattern is typical for antigens residing in or close to the glomerular

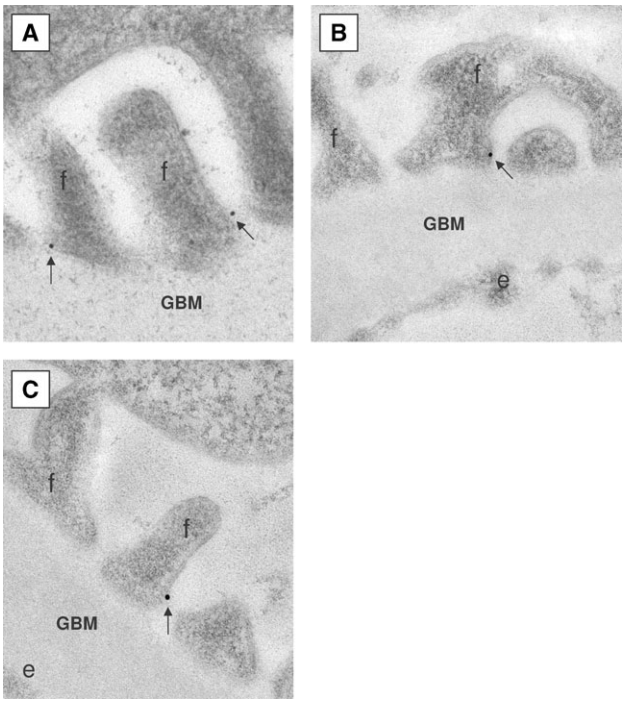

Fig. 2. Electron micrographs from three individual human kidneys (**A**–**C**), fixed with a reduced percentage of glutaraldehyde, showing the transected podocyte foot processes (f), the glomerular basal membrane (GBM) and the glomerular endothelium (e). Following incubation with a rabbit anti-CRIM1 antibody, immunolabelling was performed by incubation with 10 nm goldspheres conjugated to protein A. The majority (85%) of the spheres (arrows) were localized to the plasma membrane of the podocyte foot processes at a characteristic distance from the GBM, where the glomerular filtration slit membrane is localized. Magnification 70 000×.

basal membrane, as in the podocyte processes. The negative controls showed no staining in either of the settings, Figures 1B and 1D.

Immunoelectron microscopy

Several human kidney samples were analysed by electron microscopy following fixation in reduced amount of glutaraldehyde, showing similar results. Three of these are shown in Figure 2. In these, a total of 11 310 nm gold spheres were counted. Of these, 96 spheres (85%) were localized to the podocytes. The majority of the podocyte staining (65%, 63 spheres) was localized to the plasma membrane, more specifically to the filtration slit area of the podocyte pedicles. The remaining signal localized to the podocytes was not plasma membrane associated; instead, it was seen in the cytoplasmic compartment of the cell body of the podocyte. The distribution of the remaining labelling signal was as follows: glomerular basal membrane four spheres (3.5%), the glomerular endothelial cell five spheres (4.4%) and the cytoplasmic part of the mesangial cell eight spheres (7.1%). The tubular and interstitial compartments were negative and no staining was seen in the extraglomerular vasculature (data not shown).

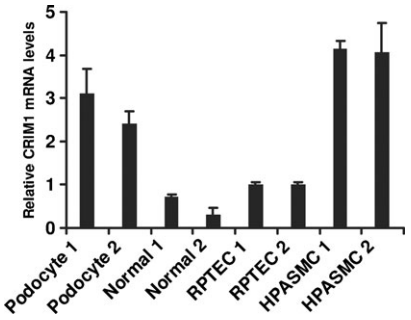

Fig. 3. Results from real-time quantitative RT-PCR assessment of CRIM1 mRNA levels in two separate cultures of conditionally immortalized podocytes (Podocytes 1 and 2), normal human kidney samples (Normal 1 and 2), primary human renal proximal tubule cells (RPTEC 1 and 2) and primary human pulmonary artery smooth muscle cells (HPASMC 1 and 2). Results are in arbitrary units ± SD. The levels were normalized to three separate housekeeping genes and the identity of the PCR product was confirmed by sequencing.

Human podocyte cell culture

The cells were of podocyte origin as judged by light microscopy, by initial characterization [20], and by positive PCR for synaptopodin, α-actinin-4, and CD2AP (data not shown).

Quantitative analysis by Q-PCR

The CRIM1 mRNA levels in immortalized human podocytes were quantitatively assessed compared to the mRNA levels from two human kidneys, primary renal proximal tubular cells and primary human pulmonary artery smooth muscle cells. The transcriptional levels were normalized to three separate house keeping genes, and the results indicate that the levels were ∼8- to 10-fold higher in the podocytes, as compared to normal kidney and 3-fold higher as compared to RPTECs. The levels in HPASMC were similar to those of the immortalized podocytes (Figure 3). The correct identity of the resulting PCR product was confirmed by sequencing.

Protein expression analysis by western blotting

The protein levels of CRIM1 in cultured podocytes during the proliferative phase and differentiation phase were similar and ∼10-fold higher than the levels of the CRIM1 protein in whole renal tissue homogenate (Figure 4).

Discussion

Proteins expressed by podocytes can be assigned to three compartments: the apical, meaning the podocyte above the plane of the slit diaphragm (SD), the basal compartment representing the part of the podocyte pedicle that is anchored to and in direct contact with the GBM and finally, the SD domain, meaning the SD proteins and the proteins associated with its insertion to the actin cytoskeleton of the foot process.

Based on animal model systems, CRIM1 seems to affect several key processes during development, particularly

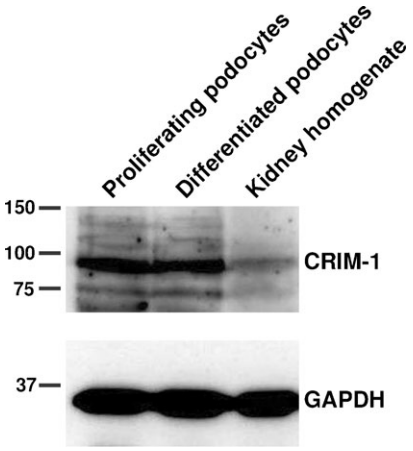

Fig. 4. Western blot analysis of CRIM1 expression in immortalized podocytes during the proliferative phase and differentiated phase as compared to the expression in renal tissue homogenate. Normalization has been performed by detecting for GAPDH. The protein levels in the podocytes is approximately ten times higher than the levels in tissue homogenate.

in the developing kidneys. A further important feature of CRIM1-disrupted mice was that proteinuria and foot-process effacement were shown to be combined with a reduction of phospho-Smad 1/5/8 levels in the mature glomerulus [5]. Phospho-Smad 1/5/8 are the downstream effectors of BMP, which indicates that the glomerular damage seen during CRIM1 disruption is at least partly due to a reduction of BMP signal transduction. Foot-process effacement and proteinuria are hallmarks of podocyte damage and indirectly; these findings implicate an ongoing CRIM1/BMP signalling activity in the mature podocyte, where CRIM1 may be essential for maintaining the BMP signalling intensity, the reduction of which may lead to foot process effacement and proteinuria.

This is, to our knowledge, the first study showing that the plasma membrane protein CRIM1 is localized mainly to the podocytes of the adult human kidney. Using both immunofluorescence and immunohistochemistry, a granular-linear staining pattern could be visualized, which is typical for proteins close to or associated with the GBM. At the ultrastructural level, it is further demonstrated by iEM that CRIM1 is localized to the SD region of the podocyte pedicles. This membrane-like structure spanning the gap between the podocyte foot processes was demonstrated by electron microscopy in 1974 [25]. For years, the exact properties of the SD were only a subject for speculation; today it has, however, been shown that the SD plays a pivotal role in the permselectivity of the kidney.

The glomerular filtration barrier consists of fenestrated endothelial cells, the glomerular basal membrane (GBM) and the SD of the podocytes [26]. Whereas the endothelium and GBM impart charge selectivity, the GBM and especially the SD impart size and shape selectivity. The basis for the permselectivity is the highly ordered net-like SD structure. Current research is rapidly shedding light on the molecular composition of the diaphragm, which has been shown to be a zipper-like structure composed of seven major proteins, the first of which to be discovered was nephrin, providing the backbone of the structure [27]. The interest in the SD has been spurred by the fact that genetic defects in one of the core proteins results in the hallmark of renal disease, namely proteinuria [27–32]. A prototypical example is the Finnish-type congenital nephrotic syndrome, where the nephrin gene has been mutated, resulting in intrauterine massive proteinuria [32].

In the adult human kidney, the tubular, interstitial and vascular compartments, lacked CRIM1 expression as judged by immunohistochemistry. This is at odds with the results of Pennisi *et al*. who showed that in mice a strong CRIM1 expression was seen in the afferent arteriole and renal vasculature [4]. We addressed this discrepancy in two ways. Commercially available antisera specified for immunohistochemical detection of CRIM1 in humans are scarce. We tested a rabbit antibody, obtained from Atlas antibodies that gave a positive glomerular staining pattern. We also obtained a chicken antibody developed for histology, developed by the human proteome resource project (www.hpr.se), obtaining an identical result. Furthermore, we tested antisera from Santa Cruz and R & D systems that, however, were specified for western blotting purposes. Both of these gave negative results, also in human placenta that was used as a positive control. Using Q-PCR, we showed that the mRNA levels of CRIM1 were ∼10-fold higher in podocytes as compared to renal cortical RNA. We also included mRNA from primary human pulmonary artery smooth muscle cells in order to assess if CRIM1 is indeed expressed in vascular smooth muscle. The results indirectly reconcile those of Pennisi *et al*. in that mRNA levels similar to the podocyte levels were present (Figure 3). The histological and PCR results may be interpreted either as a species difference between man and mouse regarding CRIM1 expression, or that the CRIM1 antigen is blocked from detection in human renal tissue vasculature. Furthermore, the presence of CRIM1 mRNA in HPASMC indicates that CRIM1 has functions during the growth and maintenance of vascular smooth muscle.

In order to ultrastructurally determine the location of CRIM1, iEM was performed demonstrating that the majority of signal was localized to the podocytes, more specifically to the filtration slit compartment. Some signal was detected in the cytoplasm of the podocyte's apical compartment. We interpret the cytoplasmic signal as CRIM1 being synthesized, or as being part of an intracellular pool of CRIM1 retaining its ligands, as CRIM1 has been shown to interact in an antagonistic way with BMP2, 4 and 7 in the cytoplasmic compartment of COS-7 cells [2].

The actual function of CRIM1 in the adult podocyte remains to be elucidated. The known CRIM1 ligands, BMP2, 4 and 7, are expressed by the podocytes during nephrogenesis [33]. Homozygous knock-out of BMP2 and four results in embryonic death during early gastrulation, while heterozygotes display severe genitourinary malformations and hypoplastic kidneys [34,35]. Homozygous disruption of the BMP7 gene results in arrested renal development and perinatal death of the litter [36]. The phenotype of the BMP7-deleted mice parallels the phenotype seen in mice where the wild-type CRIM1 has been replaced by a hypomorph version [4,5]. With regard to the presence of BMP isoforms in the adult kidney, the distribution of BMP7 has been shown

to be localized mainly to the distal tubules [18], although another study showed the presence of BMP7 in the mature podocytes of the mouse glomerulus [37]. Of the other two BMP ligands presently known to bind CRIM1, BMP2 has been shown to be downregulated in the adult kidney, whereas the distribution of BMP4 is still unknown [17,38]. Since the picture is not entirely clear, the BMP expression of adult glomerular cells requires further investigation. It is possible that CRIM1 takes part in the release of BMP for the localized paracrine interaction with the podocyte. Sequestration of members of the TGF-β superfamily, such as BMP 2, 4 and 7 to the vicinity of the SD, might implicate that the integrity of the SD is dependent upon a localized presence of these agents and that local fluctuations in concentration could be detrimental for the integrity of the SD. VEGFA is a factor that podocytes express throughout life [19,39]. Recently, CRIM1 has been shown to be involved in the delivery of VEGFA to the glomerular endothelial cells and furthermore, the localization of VEGFA as determined by electron microscopy was shown to be quite similar to the CRIM1 localization presented in the present paper, indicating a possible site for interaction [5]. It has also been demonstrated that anti-VEGF therapy and soluble flt-1 treatment leads to foot-process effacement, nephrin downregulation and glomerular endothelial damage [40]. In a recent study, it was shown that podocytes regulate the expression of podocin and its interaction with CD2AP by an autocrine VEGFA-dependent system [41]. These findings imply another important function of CRIM1 as a modulator of VEGFA action, which if disturbed, also leads to the common endpoint of foot process effacement and proteinuria.

It could also be speculated that one function of CRIM1 is to act as a sensor for the levels of its agonists, conveying the information to the segment of podocyte directly involved in the insertion and maintenance of the SD. This function of CRIM1 obviously requires an intracellular signal transductory apparatus, the existence of which is uninvestigated. A third possibility for the strict compartmentalization of CRIM1 to the SD could be a structural function of the extracellular part of the protein, in some way interacting with the slit membrane itself, adding to the structural integrity of the SD. The seven major molecules of the SD are all implicated in the structural integrity of the SD [27]. CRIM1, however, is not ascribed a structural function or a function associated with the connection of the SD to the actin cytoskeleton of the podocyte. The question is how the podocyte brings about this compartmentalization of the CRIM1 protein, since it is not known to interact with the cytoskeleton. This might be possible by the action of the lipid rafts that have been shown to be involved in the functional organization of the SD [42]. By specialization of the membrane around the SD, a means for the selective clustering of membrane proteins is obtained, in turn, providing a framework for various processes such as endocytosis, cell adhesion and signal transduction events [43,44].

Summing up, we propose that CRIM1 may be added to the list of proteins that make up the SD. Future studies could be conducted using conditional knock-out of CRIM1 in podocytes and also by molecular dissecting using isolated podocytes for *in vitro* studies.

Acknowledgements. The excellence of the technical assistance of Ms Elise Nilsson is gratefully acknowledged. This work was funded by grants from Njurfonden, the Gunnar Nilsson Cancer Foundation, Malmö University Hospital Research and Cancer Funds and the Local ALF foundation.

Conflict of interest statement. None declared.

References

1. Kolle G, Georgas K, Holmes GP *et al*. CRIM1, a novel gene encoding a cysteine-rich repeat protein, is developmentally regulated and implicated in vertebrate CNS development and organogenesis. *Mech Dev* 2000; 90: 181–193
2. Wilkinson L, Kolle G, Wen D *et al*. CRIM1 regulates the rate of processing and delivery of bone morphogenetic proteins to the cell surface. *J Biol Chem* 2003; 278: 34181–34188
3. Kinna G, Kolle G, Carter A *et al*. Knockdown of zebrafish CRIM1 results in a bent tail phenotype with defects in somite and vascular development. *Mech Dev* 2006; 123: 277–287
4. Pennisi DJ, Wilkinson L, Kolle G *et al*. Crim1KST264/KST264 mice display a disruption of the CRIM1 gene resulting in perinatal lethality with defects in multiple organ systems. *Dev Dyn* 2007; 236: 502–511
5. Wilkinson L, Gilbert T, Kinna G *et al*. Crim1KST264/KST264 Mice Implicate CRIM1 in the regulation of vascular endothelial growth factor-A activity during glomerular vascular development. *J Am Soc Nephrol* 2007; 18: 1697–1708
6. Kolle G, Jansen A, Yamada T *et al*. In ovo electroporation of CRIM1 in the developing chick spinal cord. *Dev Dyn* 2003; 226: 107–111
7. Georgas K, Bowles J, Yamada T *et al*. Characterisation of CRIM1 expression in the developing mouse urogenital tract reveals a sexually dimorphic gonadal expression pattern. *Dev Dyn* 2000; 219: 582–587
8. Glienke J, Sturz A, Menrad A *et al*. CRIM1 is involved in endothelial cell capillary formation *in vitro* and is expressed in blood vessels *in vivo*. *Mech Dev* 2002; 119: 165–175
9. Francois V, Solloway M, O'Neill JW *et al*. Dorsal-ventral patterning of the drosophila embryo depends on a putative negative growth factor encoded by the short gastrulation gene. *Genes Dev* 1994; 8: 2602–2616
10. Piccolo S, Sasai Y, Lu B *et al*. Dorsoventral patterning in Xenopus: inhibition of ventral signals by direct binding of chordin to BMP-4. *Cell* 1996; 86: 589–598
11. Schmidt J, Francois V, Bier E *et al*. Drosophila short gastrulation induces an ectopic axis in Xenopus: evidence for conserved mechanisms of dorsal-ventral patterning. *Development* 1995; 121: 4319–4328
12. Sasai Y, Lu B, Steinbeisser H *et al*. Xenopus chordin: a novel dorsalizing factor activated by organizer-specific homeobox genes. *Cell* 1994; 79: 779–790
13. Yanagita M, Oka M, Watabe T *et al*. USAG-1: a bone morphogenetic protein antagonist abundantly expressed in the kidney. *Biochem Biophys Res Commun* 2004; 316: 490–500
14. Bottinger EP. TGF-beta in renal injury and disease. *Semin Nephrol* 2007; 27: 309–320
15. Zeisberg M, Hanai J, Sugimoto H *et al*. BMP-7 counteracts TGF-beta1-induced epithelial-to-mesenchymal transition and reverses chronic renal injury. *Nat Med* 2003; 9: 964–968
16. Zeisberg M, Bottiglio C, Kumar N *et al*. Bone morphogenic protein-7 inhibits progression of chronic renal fibrosis associated with two genetic mouse models. *Am J Physiol Renal Physiol* 2003; 285: F1060–1067
17. Simic P, Vukicevic S. Bone morphogenetic proteins in development and homeostasis of kidney. *Cytokine Growth Factor Rev* 2005; 16: 299–308
18. Wetzel P, Haag J, Campean V *et al*. Bone morphogenetic protein-7 expression and activity in the human adult normal kidney is predominantly localized to the distal nephron. *Kidney Int* 2006; 70: 717–723
19. Simon M, Grone HJ, Johren O *et al*. Expression of vascular endothelial growth factor and its receptors in human renal ontogenesis and in adult kidney. *Am J Physiol* 1995; 268: F240–F250

20. Saleem MA, O'Hare MJ, Reiser J *et al*. A conditionally immortalized human podocyte cell line demonstrating nephrin and podocin expression. *J Am Soc Nephrol* 2002; 13: 630–638
21. Hultenby K, Reinholt FP, Oldberg A *et al*. Ultrastructural immunolocalization of osteopontin in metaphyseal and cortical bone. *Matrix* 1991; 11: 206–213
22. Wernerson A, Duner F, Pettersson E *et al*. Altered ultrastructural distribution of nephrin in minimal change nephrotic syndrome. *Nephrol Dial Transplant* 2003; 18: 70–76
23. Weibel E. Stereological methods. In: *Practical Methods for Biological Morphometry*. London: Academic, 1979
24. De Preter K, Speleman F, Combaret V *et al*. Quantification of MYCN, DDX1, and NAG gene copy number in neuroblastoma using a real-time quantitative PCR assay. *Mod Pathol* 2002; 15: 159–166
25. Rodewald R, Karnovsky MJ. Porous substructure of the glomerular slit diaphragm in the rat and mouse. *J Cell Biol* 1974; 60: 423–433
26. Haraldsson B, Sorensson J. Why do we not all have proteinuria? An update of our current understanding of the glomerular barrier. *News Physiol Sci* 2004; 19: 7–10
27. Mundel P, Shankland SJ. Podocyte biology and response to injury. *J Am Soc Nephrol* 2002; 13: 3005–3015
28. Benzing T. Signaling at the slit diaphragm. *J Am Soc Nephrol* 2004; 15: 1382–1391
29. Akhtar M, Al Mana H. Molecular basis of proteinuria. *Adv Anat Pathol* 2004; 11: 304–309
30. Barisoni L, Kopp JB. Update in podocyte biology: putting one's best foot forward. *Curr Opin Nephrol Hypertens* 2003; 12: 251–258
31. Chugh SS, Kaw B, Kanwar YS. Molecular structure-function relationship in the slit diaphragm. *Semin Nephrol* 2003; 23: 544–555
32. Tryggvason K. Unraveling the mechanisms of glomerular ultrafiltration: nephrin, a key component of the slit diaphragm. *J Am Soc Nephrol* 1999; 10: 2440–2445
33. Godin RE, Robertson EJ, Dudley AT. Role of BMP family members during kidney development. *Int J Dev Biol* 1999; 43: 405–411
34. Winnier G, Blessing M, Labosky PA *et al*. Bone morphogenetic protein-4 is required for mesoderm formation and patterning in the mouse. *Genes Dev* 1995; 9: 2105–2116
35. Zhang H, Bradley A. Mice deficient for BMP2 are nonviable and have defects in amnion/chorion and cardiac development. *Development* 1996; 122: 2977–2986
36. Dudley AT, Lyons KM, Robertson EJ. A requirement for bone morphogenetic protein-7 during development of the mammalian kidney and eye. *Genes Dev* 1995; 9: 2795–2807
37. Dudley AT, Robertson EJ. Overlapping expression domains of bone morphogenetic protein family members potentially account for limited tissue defects in BMP7 deficient embryos. *Dev Dyn* 1997; 208: 349–362
38. Ozkaynak E, Schnegelsberg PN, Jin DF *et al*. Osteogenic protein-2. A new member of the transforming growth factor-beta superfamily expressed early in embryogenesis. *J Biol Chem* 1992; 267: 25220–25227
39. Tufro A. VEGF spatially directs angiogenesis during metanephric development in vitro. *Dev Biol* 2000; 227: 558–566
40. Sugimoto H, Hamano Y, Charytan D *et al*. Neutralization of circulating vascular endothelial growth factor (VEGF) by anti-VEGF antibodies and soluble VEGF receptor 1 (sFlt-1) induces proteinuria. *J Biol Chem* 2003; 278: 12605–12608
41. Guan F, Villegas G, Teichman J *et al*. Autocrine VEGF-A system in podocytes regulates podocin and its interaction with CD2AP. *Am J Physiol Renal Physiol* 2006; 291: F422–F428
42. Simons M, Schwarz K, Kriz W *et al*. Involvement of lipid rafts in nephrin phosphorylation and organization of the glomerular slit diaphragm. *Am J Pathol* 2001; 159: 1069–1077
43. Simons K, Toomre D. Lipid rafts and signal transduction. *Nat Rev Mol Cell Biol* 2000; 1: 31–39
44. Cherukuri A, Dykstra M, Pierce SK. Floating the raft hypothesis: lipid rafts play a role in immune cell activation. *Immunity* 2001; 14: 657–660

Received for publication: 14.5.08; Accepted in revised form: 11.12.08

Nephrol Dial Transplant (2009) 24: 2044–2051
doi: 10.1093/ndt/gfn758
Advance Access publication 14 January 2009

Glomerular filtration is normal in the absence of both agrin and perlecan–heparan sulfate from the glomerular basement membrane

Seth Goldberg[1], Scott J. Harvey[1], Jeanette Cunningham[1], Karl Tryggvason[2] and Jeffrey H. Miner[1]

[1]Renal Division, Department of Internal Medicine, Washington University School of Medicine, St Louis, MO 63110, USA and
[2]Division of Matrix Biology, Department of Medical Biochemistry and Biophysics, Karolinska Institute, 171 77 Stockholm, Sweden

Correspondence and offprint requests to: Jeffrey H. Miner; E-mail: minerj@wustl.edu

Abstract

Background. For several decades, it has been thought that the glomerular basement membrane (GBM) provides a charge-selective barrier for glomerular filtration. However, recent evidence has presented challenges to this concept: selective removal of heparan sulfate (HS) moieties that impart a negative charge to the GBM causes little if any increase in proteinuria. Removal of agrin, the major GBM HS-proteoglycan (HSPG), from the GBM causes a profound reduction in the glomerular anionic charge without changing the excretion of a negatively charged tracer. Perlecan is another HSPG present in the GBM, as well as in the mesangium and Bowman's capsule, that could potentially contribute to a charge barrier in the absence of agrin.

Methods. Here we studied the nature of the glomerular filtration barrier to albumin in mice lacking the HS chains of perlecan either alone or in combination with podocyte-specific loss of agrin.